Colossal thermal-mechanical actuation via phase transition in single-crystal VO_2 microcantilevers

Jinbo Cao,[1,2] Wen Fan,[1,3] Qin Zhou,[4] Erica Sheu,[1] Aiwen Liu,[1] C. Barrett,[1,2] and J. Wu[1,2,a)]
[1]Department of Materials Science and Engineering, University of California, Berkeley, California 94720, USA
[2]Materials Sciences Division, Lawrence Berkeley National Laboratory, Berkeley, California 94720, USA
[3]Department of Thermal Science and Energy Engineering, University of Science and Technology of China, Hefei 230026, China
[4]Department of Mechanical Engineering, University of California, Berkeley, California 94720, USA

(Received 27 July 2010; accepted 12 September 2010; published online 28 October 2010)

The spontaneous strain associated with the structural change in the metal-insulator transition in VO_2 is orders of magnitude higher than thermal expansion mismatch used in bimetallic strips. Here we show that this strain can be leveraged to thermally activate bending of crystalline VO_2-based bilayer microcantilevers at extremely large curvatures, making them suitable for thermal sensors, energy transducers and actuators with unprecedented sensitivities. The single-crystallinity, deposition conditions, and postdeposition treatments were utilized to control the metal-insulator domain structure along the cantilever, by which we achieved bending curvatures a few hundred times higher than conventional bilayer cantilevers with the same geometry. © *2010 American Institute of Physics*. [doi:10.1063/1.3501052]

I. INTRODUCTION

Thermally activated sensors and actuators are widely used in microelectromechanical systems for modern technologies. The most common design of such devices is a bilayer strip in which two materials with different thermal expansion coefficients are mechanically coupled together. The bilayer structure bends in response to a temperature change, transducing thermal energy to mechanical motion.[1] Enhancing the bending curvature over targeted temperature change is essential for the maximal sensitivity in applications. The bending curvature depends on the thickness, elastic modulus, and more importantly, the difference in thermal expansion coefficient of the two materials $\Delta\alpha=\alpha_1-\alpha_2$. For current metal/ceramic design, $\Delta\alpha$ is on the order of 10^{-5} K^{-1}. It has been recently demonstrated that $\Delta\alpha$ can be increased up to 10^{-4} K^{-1} in organic-inorganic structures such as polymer-silicon bilayer cantilevers.[2,3] On the other hand, spontaneous strain associated with first-order structural phase transitions in many materials can be as large as 10^{-2} within a narrow temperature range.[4] Effective $\Delta\alpha$ in such processes would be over 10^{-3} K^{-1}, orders of magnitude higher than the design relying solely on thermal expansion mismatch. In this work, we exploit the large spontaneous strain from the metal–insulator phase transition and related domain structures in single-crystal VO_2 microbeams to achieve colossal thermal-mechanical effects in bilayer cantilevers.

VO_2 undergoes a first-order metal–insulator transition with a drastic change in electric and optical properties at $T_C=68$ °C.[4] The electronic phase transition is coupled with a structural transition from the high-temperature, tetragonal, metallic phase (rutile, R) to the low-temperature, monoclinic (M1), insulating phase. The M1 phase features a pairing of the vanadium atoms and a tilting of these pairs with respect to the tetragonal c axis (c_R).[4] This causes the specimen to expand by a spontaneous strain $\varepsilon\sim1\%$ along c_R direction compared to the R phase. In the meantime, the lattice shrinks by 0.6% and 0.1% along the tetragonal a_R-axis and b_R-axis, respectively.[4] It is demonstrated that external stress can drastically shift the transition temperature T_C following the uniaxial Clapeyron equation.[5,6] The transition is also ferroelastic and a compressive strain of $\sim2\%$ along c_R can switch it from M1 to R phase.[5] This structural transition has been employed to achieve high bending curvatures in microcantilevers where a VO_2 layer was coated onto a Si strip by pulsed laser deposition.[7] However, the effective spontaneous strain from this approach is small, on the order of 0.3%, due to the polycrystalline nature of the VO_2 overlayer where randomly oriented VO_2 grains exist along the cantilever length direction. When such layers undergo the phase transition, the strain contribution from c_R-oriented grains tends to cancel with that from a_R and b_R-oriented ones because they have opposite signs. Here we achieve much higher bending curvatures by fully exploiting the phase transition in single-crystal VO_2 microbeams specifically grown along its c_R axis. By coating these microbeams with Cr forming bilayer cantilevers, the curvature change reaches ~4000 m^{-1} K^{-1} across the phase transition, which is a few hundred times higher than that from the thermal expansion based cantilevers, and ~10 times higher than that from the polycrystalline VO_2/Si cantilevers.

II. EXPERIMENTAL DETAILS

Single-crystal VO_2 nano/microbeams were synthesized on SiO_2(100 nm)/Si surface using the vapor transport method reported previously, and characterized using optical

a)Electronic mail: wuj@berkeley.edu.

 © 2010 American Institute of Physics

Author complimentary copy. Redistribution subject to AIP license or copyright, see http://jap.aip.org/jap/copyright.jsp

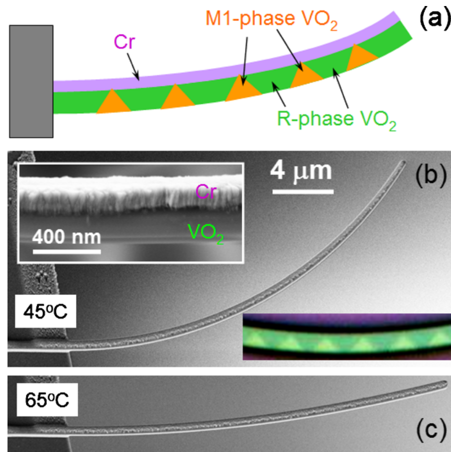

FIG. 1. (Color online) (a) Schematic view of a bilayer Cr/VO_2 cantilever. Multiple domains are created along the VO_2 beam causing continuous bending of the cantilever. (b) SEM images of a Cr/VO_2 cantilever taken at 45 °C and (c) 65 °C, respectively. Insets of (b) show magnified view of the cantilever, and an optically imaged multiple domain structure from a larger (2 μm wide) VO_2 microbeam bent to similar curvatures. Green (dark contrast)=R phase and Yellow (light contrast)=M1 phase.

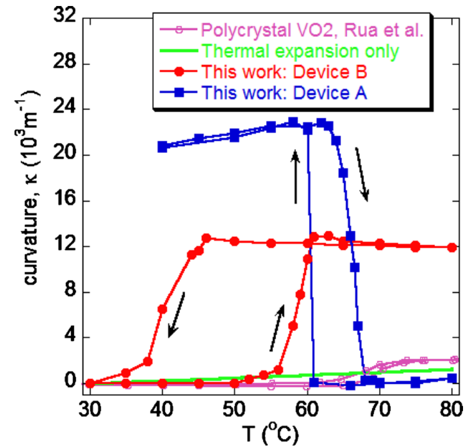

FIG. 2. (Color online) Bending curvature of two Cr/VO_2 cantilevers as a function of temperature. Also shown are data from polycrystal VO_2/Si cantilever [Rúa *et al.* (Ref. 7)] and a curve calculated for bilayer Cr/VO_2 solely with thermal expansion mismatch (i.e., excluding the phase transition).

microscopy, scanning electron microscopy (SEM), and transmission electron microscopy.[5,8] These beams grow along the c_R-axis with $\{110\}_R$ planes as bounding side faces, and have widths ranging from sub-100 nm to over micrometer and lengths from micrometer up to 100 μm.[6,8] By carefully controlling the growth condition, some of them grow out of the edge of the substrate forming cantilevers.[9] A layer of Cr was subsequently deposited onto the top surface of the cantilever using electron-beam deposition at controlled temperatures. Such Cr/VO_2 bilayer cantilevers bend in response to temperature change and the bending geometry was imaged *in situ* using optical microscope and SEM. The bending amplitude is quantified by the curvature of the bent cantilever, which is defined as the reciprocal of the bending radius R. Without phase transition, the curvature change in such a device is relatively small due to the small differential thermal expansion coefficient between Cr ($\sim 0.85\times 10^{-5}$ K^{-1}) and VO_2 ($\sim 2.0\times 10^{-5}$ K^{-1}).[10,11] On the other hand, the structural phase transition in the VO_2 layer results in much larger curvature changes as shown in Fig. 1.

III. RESULTS AND DISCUSSION

Figure 2 shows the bending curvature of two representative Cr/VO_2 cantilevers as a function of temperature. In device A, the VO_2 microbeam was coated with Cr at a temperature above its transition temperature T_C, so that it bends at low temperatures. The thicknesses of the VO_2 and Cr layers are 0.5 μm and 0.2 μm, respectively. The curvature reaches ~20 000 m^{-1} at ~40 °C. With increasing temperature, the curvature first increases slightly due to the higher thermal expansion coefficient of VO_2 than Cr. At 63 °C, the curvature shows a downward jump and vanishes at ~68 °C. This jump is a direct consequence of the 1% spontaneous strain along the cantilever length (c_R) across the phase transition in the VO_2 layer. Although the phase transition is first-order and typically occurs abruptly within less than one degree in free-standing VO_2 microbeams,[12] clamping across the Cr/VO_2 interface expands the phase transition range to ~5 °C. This is because clamping strain stabilizes a multiple M1-R domain structure along the VO_2 microbeam at intermediate temperatures, as we have previously shown,[9,12] making the phase transition gradual and effectively the second order.[13] These M1/R domains, however, line up coherently along the single-crystal VO_2 microbeam due to crystallographic restrictions of the phase transition and long-range nature of the elastic force from clamping. This domain array structure is the optimal domain configuration that minimizes the total energy of the system. Figure 1(b) inset shows such a domain array optically imaged from a VO_2 microbeam that is bent to similar curvatures by applying force to its ends. Here the microbeam is wider than those used in our cantilever experiments in order to obtain a clear optical image. The c_R (or a_{M1}) axis of the R (or M1) domains all point to the same direction (along the microbeam length),[5,6] as opposed to random directions in the polycrystalline VO_2 experiment.[7] Therefore they broaden the bending temperature range without reducing the bending amplitude. The curvature change rate is as large as 4000 m^{-1} K^{-1}, much higher than from conventional designs using metal/ceramic, polymer/silicon, or polycrystalline VO_2/silicon cantilevers as shown in Fig. 2.[2,3,7] For comparison, we calculate the contribution to the curvature change solely from thermal expansion mismatch of a Cr/VO_2 cantilever, and plot as a reference curve in Fig. 2. As expected, the curvature change from this contribution is much smaller. Note that when device A is cooled down to room temperature, the curvature change is reversible but with a ~5 °C hysteresis.

In order to investigate the effects of growth condition and postgrowth processing, we fabricated device B under different conditions. Here the Cr layer is deposited on VO_2 at a temperature below T_C so that the cantilever is straight at room temperature. The thickness of the VO_2 and Cr layers is 0.5 μm and 0.04 μm, respectively. The device was subsequently annealed at 500 °C for 2 min in order to enforce the clamping between Cr and VO_2. In opposite to device A, device B bends at high temperatures as expected. In addition, the effective transition temperature is reduced from T_C and

Author complimentary copy. Redistribution subject to AIP license or copyright, see http://jap.aip.org/jap/copyright.jsp

the hysteresis is greatly broadened. These effects are likely caused by the doping of Cr into the VO_2 microbeam at the interface during the annealing. It is known that Cr-doped VO_2 exhibits a complex phase diagram, where new monoclinic and triclinic phases can be stabilized.[14] While the exact mechanism behind these effects warrants further investigation, they point out possibilities to tune the bending behavior of the bilayer cantilevers by postfabrication thermal processing. The phase transition of device B in both heating and cooling spans a temperature range of 10–15 °C compared to that of device A at ~5 °C, making it suitable for sensing over a wider temperature range.

The curvature κ of a bilayer cantilever with rectangular cross section can be calculated from the expression[15]

$$\kappa = \frac{1}{R} = \frac{6E_1E_2t_1t_2(t_1+t_2)}{E_1^2t_1^4 + 2E_1E_2t_1t_2(2t_1^2+3t_1t_2+2t_2^2) + E_2^2t_2^4}\varepsilon, \quad (1)$$

where E_1 and E_2 are the biaxial modulus of the two materials, t_1 and t_2 are their thickness, and ε is the total axial strain developed within the temperature range. For bilayer cantilevers operating solely on differential thermal expansion, the strain $\varepsilon = \Delta\alpha \times \Delta T$ and is typically on the order of 10^{-4} for 10 °C temperature change. For VO_2-based bilayer cantilever, ε is the spontaneous strain equal to 10^{-2} along the cantilever length direction. Therefore the latter can be much more sensitive than the former for applications in narrow temperature ranges. From Eq. (1), as κ scales inversely with the thickness, thinner cantilevers can achieve higher sensitivity for sensing applications. On the other hand, for actuator applications thick cantilevers are needed to offer higher forces. For different applications these factors must be balanced in design to exploit the best potential of the cantilevers.

To further understand how the geometry affects the cantilever operation, we fabricated bilayer Cr/VO_2 cantilevers at different layer thicknesses. As the curvature κ depends on the thickness of the bilayer cantilever, we normalize the curvature of each device to the thickness of its VO_2 layer (t_1) and plot the dimensionless curvature $t_1/R\varepsilon$ as a function of the ratios of the Cr/VO_2 thickness (t_2/t_1) and Young's modulus (E_2/E_1). The inset of Fig. 3 shows such a contour plot theoretically predicted by Eq. (1). For bilayer cantilever with geometry $t_2/t_1 < 1$, it is obvious that an increase in the Young's modulus of the coating material (E_2) results in larger $t_1/R\varepsilon$. The horizontal dashed line indicates the Young's modulus ratio between Cr (~280 GPa) and VO_2 (~140 GPa).[16] The nonmonotonic dependence of $t_1/R\varepsilon$ on t_2/t_1 indicates that the thickness of the coating layer (t_2) must be carefully selected in order to maximize $t_1/R\varepsilon$. We deposited different thicknesses of Cr onto VO_2 and measured their normalized curvature change across the phase transition and plotted in Fig. 3. As can be seen in Fig. 3, the experimental data follow closely the theoretical prediction from Eq. (1). The normalized curvature is relatively small for small t_2/t_1, then rapidly increases to a maximum of ~1.0 at $t_2/t_1 = 0.37$, and slowly decreases for more Cr coating. Therefore, both too thin and too thick Cr coating would reduce $t_1/R\varepsilon$. In addition, we note that T_C of VO_2 can be rapidly reduced toward room temperature by doping with small fractions of tungsten (W).[17] Piece-wise or gradual bending of the cantilever could be achieved by doping with tungsten at graded concentration along the length or width of the VO_2 microbeam, or by coating with Cr at graded thickness. These effects provide further ways to engineer the operational sensitivity, temperature range, and bending behavior of the VO_2-based bilayer cantilevers. For example, if the VO_2 is doped with W and the W fraction x is linearly varied from 3% at the root to 0 at the tip of the cantilever, the $Cr/W_xV_{1-x}O_2$ cantilever would start to bend at room temperature from the root, and gradually complete at 68 °C at the tip, covering a wide response range of ~40 °C. These devices can be used to sense temperature changes at extremely high sensitivities with mechanical motion or optical reflection as read out.

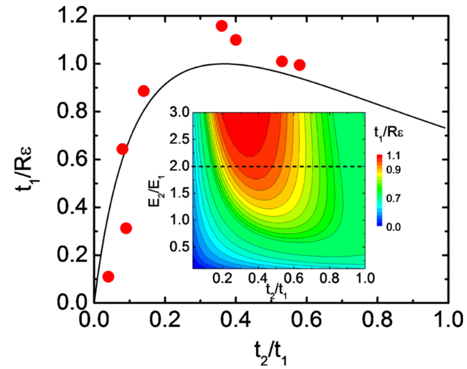

FIG. 3. (Color online) Normalized curvature for Cr/VO_2 cantilevers as a function of the bilayer thickness ratio. The solid line is calculated from Eq. (1), and the data points are from experimental results. Inset: normalized curvature of VO_2-based cantilevers as a function of Young's modulus and bilayer thickness ratios. The Young's modulus ratio between Cr and VO_2 is 2, and is shown by the dashed line and in the main panel.

IV. CONCLUSIONS

In summary, we demonstrate that the phase transition and domain structures in single-crystal VO_2 microbeams can be leveraged in bilayer cantilevers to achieve thermally activated bending at curvatures hundreds of times larger than conventional devices. Effects of geometry and deposition conditions were controlled to tune the operation temperature range and sensitivity, which show excellent agreement with theoretical predictions. As the large bending is activated by small temperature changes near room temperature, these devices may be also integrated with piezoelectrics for thermal energy harvesting at small ΔT near ambient temperatures.

ACKNOWLEDGMENTS

This work was supported by a Siemens Seed Fund at U.C. Berkeley (measurements) and by the National Science Foundation (NSF) under Grant No. EEC-0832819 (material synthesis and device fabrication).

[1] W. Riethmuller and W. Benecke, IEEE Trans. Electron Devices **35**, 758 (1988).
[2] M. C. LeMieux, M. E. McConney, Y.-H. Lin, S. Singamaneni, H. Jiang, T. J. Bunning, and V. V. Tsukruk, Nano Lett. **6**, 730 (2006).
[3] K. M. Goeders, J. S. Colton, and L. A. Bottomley, Chem. Rev. **108**, 522 (2008).

Author complimentary copy. Redistribution subject to AIP license or copyright, see http://jap.aip.org/jap/copyright.jsp

[4]V. Eyert, Ann. Phys. **11**, 650 (2002).
[5]J. Cao, E. Ertekin, V. Srinivasan, W. Fan, S. Huang, H. Zheng, J. W. L. Yim, D. R. Khanal, D. F. Ogletree, J. C. Grossman, and J. Wu, Nat. Nanotechnol. **4**, 732 (2009).
[6]J. Cao, Y. Gu, W. Fan, L. Q. Chen, D. F. Ogletree, K. Chen, N. Tamura, M. Kunz, C. Barrett, J. Seidel, and J. Wu, Nano Lett. **10**, 2667 (2010).
[7]A. Rúa, F. l. E. Fernández, and N. Sepúlveda, J. Appl. Phys. **107**, 074506 (2010).
[8]B. S. Guiton, Q. Gu, A. L. Prieto, M. S. Gudiksen, and H. Park, J. Am. Chem. Soc. **127**, 498 (2005).
[9]W. Fan, S. Huang, J. Cao, E. Ertekin, C. Barrett, D. R. Khanal, J. C. Grossman, and J. Wu, Phys. Rev. B **80**, 241105(R) (2009).
[10]D. I. Bolef and J. de Klerk, Phys. Rev. **129**, 1063 (1963).
[11]D. Kucharczyk and T. Niklewski, J. Appl. Crystallogr. **12**, 370 (1979).
[12]J. Wu, Q. Gu, B. S. Guiton, N. P. de Leon, L. Ouyang, and H. Park, Nano Lett. **6**, 2313 (2006).
[13]A. Tselev, E. Strelcov, I. A. Luk'yanchuk, J. D. Budai, J. Z. Tischler, I. N. Ivanov, K. Jones, R. Proksch, S. V. Kalinin, and A. Kolmakov, Nano Lett. **10**, 2003 (2010).
[14]M. Marezio, D. B. McWhan, J. P. Remeika, and P. D. Dernier, Phys. Rev. B **5**, 2541 (1972).
[15]S. Timoshenko, J. Opt. Soc. Am. **11**, 233 (1925).
[16]K.-Y. Tsai, T.-S. Chin, and H.-P. D. Shieh, Jpn. J. Appl. Phys., Part 1 **43**, 6268 (2004).
[17]Q. Gu, A. Falk, J. Wu, L. Ouyang, and H. Park, Nano Lett. **7**, 363 (2007).

Author complimentary copy. Redistribution subject to AIP license or copyright, see http://jap.aip.org/jap/copyright.jsp